# Involvement of the Polycomb-group gene *Ring1B* in the specification of the anterior-posterior axis in mice

**Maki Suzuki[1,2,\*], Yoko Mizutani-Koseki[1,\*], Yu-ichi Fujimura[1,\*], Hiro Miyagishima[1], Tomomi Kaneko[1], Yuki Takada[1], Takeshi Akasaka[1], Hideki Tanzawa[2], Yoshihiro Takihara[3], Megumi Nakano[4], Hiroshi Masumoto[4], Miguel Vidal[5], Kyo-ichi Isono[1] and Haruhiko Koseki[1,6,†]**

[1]Department of Molecular Embryology, Graduate School of Medicine, Chiba University, 1-8-1 Inohana, Chuo-ku, Chiba 260-8670, Japan
[2]Department of Oral Surgery, Graduate School of Medicine, Chiba University, 1-8-1 Inohana, Chuo-ku, Chiba, 260-8670, Japan
[3]Department of Develomental Biology and Medicine, Osaka Medical Center for Cancer and Cardiovascular Diseases, Nakamiti 1-3-3, Tousei-ku, Osaka, 537-8511, Japan
[4]Division of Biological Science, Graduate School of Science, Nagoya University, Furo-cho, Chikusa-ku, Nagoya, 464-8602 Japan
[5]Centro de Investigaciones Biologicas, Department of Developmental and Cell Biology, Velazquez 144, 28006 Madrid, Spain
[6]RIKEN Research Center for Allergy and Immunology, 1-7-22 Suehiro, Tsurumi-ku, Yokohama 230-0045, Japan
*These authors contributed equally to this work
†Author for correspondence (e-mail: koseki@med.m.chiba-u.ac.jp)

## SUMMARY

The products of the Polycomb group of genes form complexes that maintain the state of transcriptional repression of several genes with relevance to development and in cell proliferation. We have identified Ring1B, the product of the *Ring1B* gene (*Rnf2* – Mouse Genome Informatics), by means of its interaction with the Polycomb group protein Mel18. We describe biochemical and genetic studies directed to understand the biological role of Ring1B. Immunoprecipitation studies indicate that Ring1B form part of protein complexes containing the products of other Polycomb group genes, such as Rae28/Mph1 and M33, and that this complexes associate to chromosomal DNA. We have generated a mouse line bearing a hypomorphic *Ring1B* allele, which shows posterior homeotic transformations of the axial skeleton and a mild derepression of some Hox genes (*Hoxb4*, *Hoxb6* and *Hoxb8*) in cells anterior to their normal boundaries of expression in the mesodermal compartment. By contrast, the overexpression of Ring1B in chick embryos results in the repression of *Hoxb9* expression in the neural tube. These results, together with the genetic interactions observed in compound *Ring1B*/*Mel18* mutant mice, are consistent with a role for Ring1B in the regulation of Hox gene expression by Polycomb group complexes.

Key words: Polycomb, Ring1B, Mel18, Hox, Mouse

## INTRODUCTION

The Polycomb group (PcG) of genes was first identified by their requirement for the maintenance of the stable repression of Hox genes during the development of *Drosophila melanogaster* (Paro, 1995; Pirotta, 1997). Biochemical and immunohistochemical analyses indicate that *Drosophila* PcG gene products function as large multimeric protein complexes that are thought to act by changing the local chromatin structure (Paro, 1995; Pirotta, 1997). Synergistic genetic interactions between mutant alleles of different *Drosophila* PcG genes indicate their ability to affect the expression of Hox genes in a gene dose-dependent manner and are in line with the action of PcG gene products in multimeric protein complexes (Jurgens, 1985; Franke et al., 1992; Shao et al., 1999).

Mammalian genes that are structurally and functionally related to *Drosophila* PcG genes have been identified. The PcG gene products form parts of two different complexes. One complex contains the product of *Eed* (the ortholog of the *Drosophila extra sex combs* gene), and the products of *Enx1* (Ezh2 – Mouse Genome Informatics) and *Enx2* (the orthologs of the *Drosophila enhancer of zeste* gene). Eed interacts with histone deacetylases (Schumacher et al., 1996; Laible et al., 1997; van Lohuizen et al., 1998; Sewalt et al., 1998; van der Vlag and Otte, 1999). The second complex include the products of the paralogs of a subset of PcG genes. These genes exist as gene groups like *Mel18* (Zfp144 – Mouse Genome Informatics) and *Bmi1*; *M33* (Cbx2 – Mouse Genome Informatics), *Mpc2* (Cbx4 – Mouse Genome Informatics) and *Pc3* (*Cbx8* – Mouse Genome Informatics); Rae28 (*Edr1* – Mouse Genome Informatics)/*Mph1* and Mph2 (*Edr2* – Mouse Genome Informatics); and *Ring1A* (*Ring1* – Mouse Genome Informatics) and *Ring1B* (*Rnf2* – Mouse Genome Informatics) (Tagawa et al., 1990; van Lohuizen et al., 1991; Pearce et al., 1992; Satijn et al., 1997a; Hemenway et al., 2000; Nomura et al., 1994; Gunster et al., 1997; Schoorlemmer et al., 1997; Satijn et al., 1997b; Hemenway et al., 1998). This complex is

similar to the Polycomb repressive complex 1 (PRC1) recently identified in *Drosophila* (Shao et al., 1999; Gebuhr et al., 2000). Indeed, mice bearing mutations in *Mel18*, *Bmi1*, *M33*, *Mph1* or *Ring1A* show homeotic transformations of the axial skeleton and alterations in the expression patterns of Hox genes (Akasaka et al., 1996; van der Lugt et al., 1994; Core et al., 1997; Takihara et al., 1997; del Mar Lorente et al., 2000). Interestingly, *Ring1A* mutants exhibit anterior transformations, while the others show posterior transformations (del Mar Lorente et al., 2000). In addition, mice with compound mutations in these genes show synergistic enhancement of the phenotypes associated with the individual genes evidencing genetic interactions between these mutations (Bel et al., 1998; Akasaka et al., 2001). This complex is required for the maintenance of the stable repression of Hox genes, as indicated by progressive derepressions of *Hoxb3* expression in migrating facial neural crest cells in *Mel18*/*Bmi1* compound and *Rae28*/*Mph1* mutant embryos (Tomotsune et al., 2000; Akasaka et al., 2001).

To gain further insight in mammalian PcG function, we searched for Mel18 interactors and found Ring1B. The Ring1B protein is closely related to the product of PcG gene Ring1A, and was first identified by its interaction with the product of M33 (Schoorlemmer et al., 1997). Ring1B was also found to interact with Bmi1 and Mph2 in yeasts (Hemenway et al., 1998). Here we provide evidence for the presence of Ring1B in a complex containing *M33*, *Mel18* and *Rae28*/Mph1 in extracts prepared from 11.5 days post coitus (dpc) mouse embryo, which were found associated to chromosomal DNA. These observations strongly suggest that Ring1B is a component of the mammalian counterpart of *Drosophila* PRC1 complex, as *Drosophila* Ring protein is included in PRC1 (Saurin et al., 2001). To test this possibility functionally, we attempted to generate a loss-of-function mouse model for *Ring1B*. Here, we describe a mouse line bearing a hypomorphic mutation for *Ring1B* and show that this mutation is accompanied by limited homeotic transformations of the axial skeleton and alterations in Hox gene expression. In addition, we show a genetic interaction between the *Ring1B* and *Mel18* mutations. We also performed a gain-of-function experiment by in ovo electroporation. Overexpression of Ring1B protein in the developing neural tube results in the repression of chick *Hoxb9* expression. These results demonstrate that Ring1B plays a role in the anteroposterior (AP) specification of the paraxial mesoderm and neural tube in vertebrate embryos.

## MATERIALS AND METHODS

### Yeast two hybrid assay

A *Mel18* full-length cDNA was fused in-frame to the *lexA*-coding sequence in vector pBTM116 (Fields and Bartel, 2001). The L40 yeast strain containing *lexA-HIS3* and *lexA-lacZ* reporter genes was first transformed with pBTM116-*Mel18*, and then with the mouse 11.0 dpc embryo Matchmaker cDNA library in pGAD10 (Gal4 activation domain fusion vector, Clontech), using the lithium acetate method. Six hundred independent colonies were isolated from $7 \times 10^6$ transformants on selective media plate lacking leucine, tryptophan and histidine and supplemented with 5 mM 3-aminotriazole. All these clones were restreaked onto the selection media and assayed for β-galactosidase activity by a filter assay (Vojtek et al., 1993). cDNA

fragments were amplified by direct colony PCR from the His+*lacZ*+ positive clones, identified by sequencing and searched for using NCBI similarity search programs (BLASTn). Twenty clones, which were possible interactors of Mel18, were cured of the LexA fusion plasmid by growth on synthetic medium lacking leucine. Plasmid loss was confirmed by plating on both Leu-, Trp+ and Leu-, trp- plates. The selected clones grew only on trp+ media. The plasmid DNA was then prepared from those positive clones of interest and transformed into *E. coli* DH5α.

To test for interaction specificity, each pGAD10 variant containing *Mel18*, *Bmi1*, *Ring1A*, *Ring1B*, *Mph2* or lamin was transformed into L40 (MATa), and each pBTM116 variant containing *Mel18*, *Bmi1*, *Ring1A*, *Ring1B* or *Mph2* was transformed into AMR70 (MATα). Then the transformed clones were mated to each other in all possible combinations on YPAD plates. The Leu+Trp+ diploids were selected on Leu-Trp- plate and assayed for β-galactosidase activity using a filter assay.

### *In vitro* transcription/translation and GST pull-down assay

The full-length and deleted *Mel18* and *Ring1B* cDNAs were subcloned in the pcDNA3 vector (Invitrogen Japan, Tokyo, Japan). RNA was synthesized with 500 ng of supercoiled plasmids and translated in the presence of 10 μCi of [$^{35}$S] methionine (Amersham Biosciences, Tokyo, Japan) using the TNT T7 Quick Coupled Reticulocyte Lysate System (Promega, Tokyo, Japan). Ten micrograms of plasmids containing GST fused to either intact or truncated Mel18 or Ring1B cDNAs or GST alone (as a negative control) were pre-bound to 10 μl of a 1:1 suspension of Glutathion Sepharose 4 Fast Flow (Amersham Biosciences, Tokyo, Japan) and then incubated on a rotating wheel with the in vitro translation mixture in 500 μl of NETN buffer (0.5% NP-40, 20 mM Tris-Cl pH 8.0, 11 mM NaCl, 1 mM EDTA and 100 mM PMSF) for 1 hour at 4°C Bound proteins were eluted by boiling in SDS sample buffer and were analyzed on 11% polyacrylamide gels. Gel images were obtained by BAS-2000II Bio-Imaging Analyzer (FUJIFILM, Tokyo, Japan).

### Antibodies

The following antibodies were used in this study:
mouse anti-mouse Ring1B monoclonal antibody (clone 3) (Atsuta et al., 2001);
rabbit anti-mouse Ring1B antiserum (Garcia et al., 1999);
rabbit anti-mouse Ring1A antiserum (Schoorlemmer et al., 1997);
mouse anti-mouse Rae28/Mph1 monoclonal antibody (K. I., H. M. and H. K., unpublished);
rabbit anti-mouse Rae28/Mph1 antiserum (Y. T., unpublished);
goat anti-mouse Mel18 purchased from Santa Cruz Biotechnology (Santa Cruz Biotechnology, Santa Cruz, CA);
mouse anti-mouse Bmi1 monoclonal antibody (Alkema et al., 1997);
rabbit anti-mouse M33 antiserum (Schoorlemmer et al., 1997);
rabbit anti-demethyl-HistoneH3 antiserum (Upstate Biotechnology, Lake Placid, NY) (Nakayama et al., 2001);
mouse anti-Bip monoclonal antibody (StressGen Biotechnologies, Victoria, B.C., Canada);
goat anti-Lamin B antibody (Santa Cruz Biotechnology, Santa Cruz, CA);
anti-HA epitope monoclonal antibody (Santa Cruz Biotechnology, Santa Cruz, CA);
rabbit anti-CENP-B antibody (BN1) (Kitagawa et al., 1995); and
goat anti-centromeric antigen (ACA) antiserum (Yoda et al., 1996).

### Immunoprecipitations and western blot analysis

Total cellular extracts were prepared from 11.5 dpc mouse embryos. A single embryo was solublized by sonication in 1 ml of TE (10 mM Tris-HCl, pH 8.0, 1 mM EDTA) using a Handy Sonic model UR-20P (TOMY seiko, Tokyo, Japan) followed by centrifugation at 9100 *g* for 5 minutes at 4°C to remove insoluble material. For immunoprecipitation, lysates were incubated with 1/2 volume of

hybridoma culture supernatants containing either anti-Ring1B or anti-Rae28/Mph1 monoclonal antibodies, or with 1/30 volume of anti-Mel18 antiserum for 1 hour at 4°C with rocking. Immunocomplexes were captured with Protein A Sepharose beads (Amersham). Western blotting was performed as described previously (Atsuta et al., 2001).

### Immunofluorescence staining

U2-OS human osteosarcoma cells were used for immunofluorescence staining analyses as described previously (Atsuta et al., 2001). For the analysis of mitotic cells, cells were fixed with 70% acetone at –20°C for 30 minutes and air dried. Fixed cells were incubated with blocking solution for 1 hour at room temperature, and incubated with the mixture of rabbit anti-CENP-B antibody or ACA serum (1:200 dilution) and anti-Ring1B antibody for 2 hours at 37°C. Cells were washed with phosphate-buffered saline containing 0.1% Tween 20 (PBST) for 5 minutes at room temperature four times, and then incubated with fluorescein isothiocyanate-conjugated anti-rabbit IgG (1:160 dilution) (MBL, Nagoya, Japan) or fluorescein isothiocyanate-conjugated anti-human IgG (1:160 dilution) (MBL, Nagoya, Japan) and rhodamine-conjugated anti-mouse IgG (1:200 dilution) (MBL, Nagoya, Japan) diluted with PBST supplemented with 10% fetal bovine serum at 37°C for 1 hour. Cells on coverslips were then washed four times with PBST for 5 minutes at room temperature. Chromosomal DNA was stained with DAPI (1 μg/ml). Images were obtained with a fluorescence microscope (Carl Zeiss Japan, Tokyo, Japan) equipped with a cooled-CCD camera (PXL, Photometrics, CA) and IPLab software (Signal Analytics).

### Chromatin purification by cesium chloride isopyknic centrifugation

Mouse embryos at 12.5 dpc were minced with scissors and subjected to chemical crosslinking with 1% formaldehyde in phosphate-buffered saline (PBS) for 30 minutes. Isolation of chromatin fraction was performed as described elsewhere (Orlando et al., 1997).

### Generation of a hypomorphic allele of the *Ring1B* gene

A modified *Ring1B* allele was generated by gene targeting in R1 embryonic stem (ES) cells. Genomic *Ring1B* sequences were isolated from a mouse 129/SVJ genomic library. The targeting vector contains as homology arms, an *Eco*RI-*Sac*I fragment containing two exons encoding the RING finger of Ring1B and a flanking *Eco*RI-*Hin*dIII fragment. *MC1Neo* and *HSVtk* genes were used as selectable cassettes for positive and negative selections, respectively (Fig. 6A). Thirty micrograms of the linearized plasmid were electroporated into 2×10⁷ R1 ES cells. Two hundred and forty double resistant R1 clones were analyzed by Southern blot. One of the clones showed an alteration in the *Ring1B* locus and was used to generate germline chimeras as described (Nagy et al., 1993).

### Single and double mutant mice

We generated homozygous *Ring1B* mutant mice by interbreeding heterozygous animals that had been backcrossed eight times into C57BL/6J. *Mel18*-deficient mice (Akasaka et al., 1996) from both C57BL/6J genetic background were also used in this study. *Ring1B* and *Mel18* heterozygous mice in C57BL/6J genetic background were interbred to generate compound homozygous mutant mice. Skeletal phenotypes of *Ring1B* mutants were also investigated on the compound genetic background between 129/SvJ derived from R1 ES cells and C57BL/6J. *Ring1B* and *Mel18* mutations were backcrossed onto C57BL/6J twice (N2). N2 heterozygotes were intercrossed to generate homozygous mutants. This hybrid line was maintained by brother-sister mating for at least ten generations.

 *Ring1B* mutant mice were genotyped by PCR using the following oligonucleotides (Fig. 5A): RB22, 5′-GTTGAAGACTTCATTG-TACC-3′ and RB18, 5′-GGAAGTCACATCTTAGCAGG-3′ for the *Ring1B* wild-type allele; and Neo2, 5′-CTTCCATCCGAGTAC-GTGCT-3′ and RB11, 5′-TTATCTTCTGCTCCACTACC-3′ for the

mutant allele. Oligonucleotides used for genotyping *Mel18* mutant mice have been described previously (Akasaka et al., 2001).

### Phenotypic analysis

Skeletal analysis of 18.5 dpc or new born mice and in situ hybridization to 11.5 dpc embryo sections were performed as described previously (Kessel and Gruss, 1991). *Hoxb4* from Dr R. Krumlauf, *Hoxb6* from Dr K. Schughart and *Hoxb8* from Dr J. Deschampus were used (Akasaka et al., 1996). Whole-mount in situ hybridization was performed as described previously with slight modifications (Wilkinson and Nieto, 1993). Briefly, maleic acid buffer (0.5 M maleic acid, 0.15 M NaCl, pH 7.5) was used for washes after antibody reaction. Chicken *Hoxb9* provided by Dr A. Kuroiwa, and mouse *Mel18* and *Ring1B* probes were used.

### In ovo electroporation

cDNA fragments encoding the entire ORF of mouse *Mel18* and *Ring1B* were amplified by PCR using primers that provided *Xho*I sites on both ends of the fragments for subcloning into the *Xho*I site of pCXN2 (kindly provided by Dr Jun-ichi Miyazaki, Osaka University, Japan) (Niwa et al., 1991). Empty pCXN2 vector was used as a negative control. In ovo electroporation was performed as described previously (Sakamoto et al., 1998; Nakamura and Funahashi, 2001). Expression vectors were dissolved at 2 μg/μl in PBS and mixed with 1/10 volume of 2 μg/μl β-galactosidase expression vector, pCHO110 (Amersham Biosciences, Tokyo, Japan), or green fluorescence protein (GFP) expression vector, pcDNA-GFP, and 1/20 volume of saturated Nile Blue solution. Fertilized chick eggs were purchased from Shiroyama chicken farm (Kanagawa, Japan) and cultured at 37.2°C before and after electroporation. The stages of chicken embryos were determined by counting somite number. After electroporation, embryos were re-incubated for varying length of time to allow expression of the introduced foreign DNA into one side of the neural tube and subsequently dissected and fixed in 4% paraformaldehyde in PBS.

## RESULTS

### In vitro interaction of Ring1B and Mel18

Among 63 Mel18-binding proteins identified in the screening of cDNAs from an 11.0 dpc mouse embryo library, 22, 8 and two cDNA clones encoded parts of Ring1B, Mph2 and Rae28/Mph1 proteins, respectively (T. A., unpublished). In order to asses the specificity of the interactions, we performed yeast two hybrid mating assays (Fig. 1A). Bmi1, which is known to interact with Ring1B and Mph2, was used as positive control and Lamin as a negative control (Hemenway et al., 1998). Because Ring1A, a structurally related protein to Ring1B, was never identified in our screening of Mel18 interactors, we also examined the interaction of Mel18 and Ring1A. As visualized by β-galactosidase activity, Mel18 interacted strongly with Ring1B and Mph2 but hardly with itself, Bmi1 or Ring1A in our experimental conditions.

 To determine whether the Mel18 protein can directly interact with Ring1B, we used an in vitro GST pull-down assay (Fig. 1B). Radiolabeled full-length or truncated Mel18 and Ring1B proteins were synthesized in vitro and tested for binding activity to respective GST fusion proteins with full-length Ring1B (GST-Ring1B), a C-terminal-truncated Ring1B (GST-Ring1BΔC) (amino acids 1-188), N-terminal-truncated Ring1B (GST-Ring1BΔN) (amino acids 189-365) and Mel18 lacking PEST region (GST-Mel18ΔPEST) (amino acids 1-233). Radiolabeled full-length Mel18 (Mel18fl) was able to

bind to GST-Ring1B and GST-Ring1BΔC, and weakly to GST-Ring1BΔN but exhibited no appreciable binding to GST-Sepharose alone (Fig. 1B, part a). Because we could not obtain

a full-length Mel18 protein fused to GST, we instead prepared a GST-Mel18ΔPEST protein. Full-length Ring1B (Ring1Bfl) bound to GST-Mel18ΔPEST but not to GST-Sepharose (Fig.
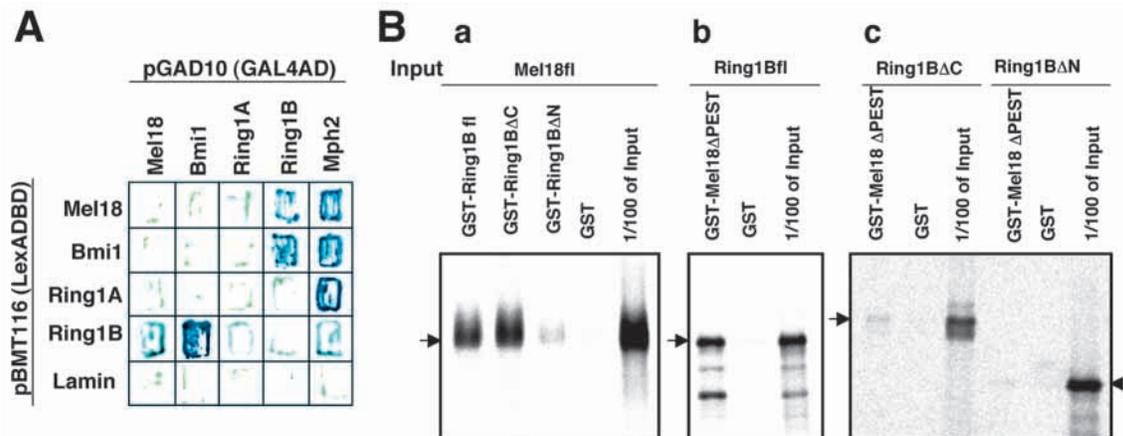


**Fig. 1.** Interactions between Ring1B and Mel18. (A) Interaction in yeast cells indicated by the β-galactosidase activity. Yeast cellswere transformed with the indicated plasmids. Lamin was a negative control. (B) GST pull-down assays. (Part a) Binding of $^{35}$S-labeled full-length Mel18 protein (Mel18fl) to GST or GST fused to either full-length or truncated Ring1B (GST-Ring1Bfl, GST-Ring1BΔC or GST-Ring1BΔN, respectively). (Part b) Binding of $^{35}$S-labeled full-length Ring1B protein (Ring1Bfl) to GST or GST fused to truncated Mel18 (GST-Mel18ΔPEST) (amino acids 1-233). (Part c) Binding of $^{35}$S-labeled truncated Ring1B proteins (Ring1BΔC and Ring1BΔN) to GST or GST-Mel18ΔPEST.
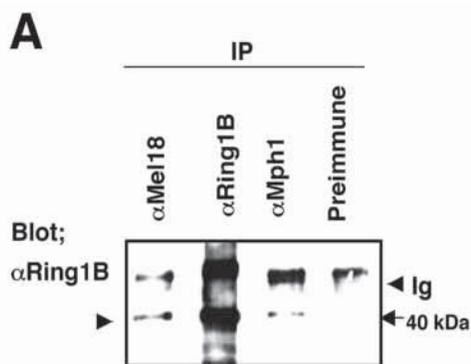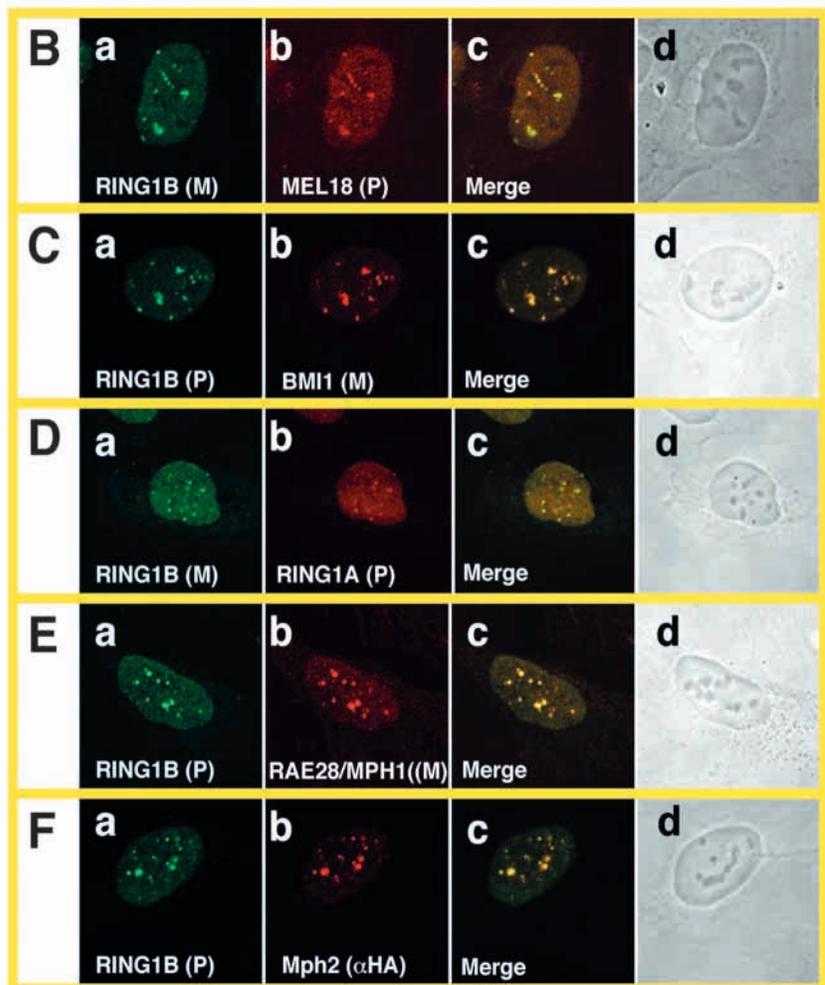


**Fig. 2.** In vivo association of Ring1B with mammalian PcG proteins. (A) Specific co-immunoprecipitation of Ring1B from 11.5 dpc mouse embryos using antibodies against Mel18 and Rae28/Mph1. The signals corresponding to the immunoglobulin heavy chains are indicated by arrowheads (Ig). (B-F) Comparative analysis of the subnuclear distributions of endogenous RING1B and MEL18 (B), BMI1 (C), RING1A (D), RAE28/MPH1 (E) and exogenous Mph2 (F) in normal or transfected human osteosarcoma U2-OS cells using indirect immunofluorescence. (Parts a) The signal of RING1B (green). (Parts b) The signals of endogenous MEL18 (B), BMI1 (C), RING1A (D), RAE28/MPH1 (E) and exogenous Mph2 (F) (red). (Parts c) Merged images. (Parts d) Phase contrast views. Monoclonal and polyclonal antibodies are indicated as M and P, respectively, in parentheses.

1B, part b). These observations indicated potential direct interaction of Mel18 and Ring1B. Ring1BΔC fragment was capable to bind to GST-Mel18ΔPEST more efficiently than Ring1BΔN fragment (Fig. 1B, part).

## In vivo interaction of Ring1B with PcG proteins

To obtain evidence for the in vivo association of Ring1B with mammalian PcG proteins in mammalian cells, we performed immunoprecipitation analysis using extracts from 11.5 dpc mouse embryos. We used anti-Mel18, anti-Ring1B or anti-Mph1 antibodies and preimmune rabbit serum as a negative control. A band with a mobility corresponding to 40 kDa was recognized with anti-Ring1B antibodies in the material immunoprecipitated by anti-Mel18, anti-Ring1B and anti-Rae28/Mph1 antibodies (Fig. 2A). This shows that protein complexes isolated from murine embryos containing Mel18 or Rae28/Mph1 also contain Ring1B.

Additional evidence for the in vivo association of Ring1B with Mel18 and other PcG proteins was obtained from their subcellular localization in U2-OS cells by indirect immunofluorescence (Fig. 2B-F). Endogenous Ring1B colocalized extensively with Mel18, Bmi1, Ring1A and Rae28/Mph1 in subnuclear speckles, previously termed PcG bodies, in interphase nuclei of U2-OS cells (Fig. 2B-E) (Saurin et al., 1998). Because a specific antibody against Mph2 was not available, we used U2-OS cells stably expressing Myc-tagged Mph2. In these cells endogenous Ring1B colocalized with Myc-tagged Mph2 (Fig. 2F). Taken together, these observations indicate that the PcG complexes in PcG bodies of interphase cells contain Ring1B.

## Binding of Ring1B-containing PcG complexes to chromosomal DNA

Evidence for the association of PcG complexes to chromosomal DNA is available only for *D. melanogaster* (Zink and Paro, 1989; Orlando and Paro, 1993). To see whether mouse PcG complexes are also associated with chromosomal DNA, we analyzed formaldehyde crosslinked embryonic tissues after fractionation by cesium chloride isopyknic centrifugation for the presence of PcG proteins. Coomassie Brilliant Blue G-250 (CBB) staining showed most of the protein in fractions 1 to 3 but also in fractions 4 to 8 (Fig. 3B), whereas most chromosomal DNA was in fractions 5 to 7 (Fig. 3A). As a control, we studied the distribution of Bip, a luminal protein in the endoplasmic reticulum (ER) and nuclear envelope, which is thought not to interact with chromosomal DNA (Gething, 1999). The results showed that Bip was found in fractions 1 to 4, but it was absent from fractions 5 to 7 (Fig. 3C). A similar observation was obtained for Grp78, another ER luminal protein (Y. F., unpublished) (Gething, 1999). From the reciprocal distribution of chromosomal DNA and ER luminal proteins, we conclude that fractions 5 to 7 contain most of the chromatin-associated proteins. Distribution of dimethyl-Histone H3 to fractions 5 to 7 but not to fractions 1 and 2 revealed its similar distribution to chromosomal DNA (Fig. 3D) (Nakayama et al., 2001). This suggests that proteins that are not associated with chromatin are mainly distributed into fractions 1 and 2. Western blot analysis of these fractions showed that Ring1B and M33 were present in fractions 1 to 6 and Rae28/Mph1 in fractions 1 to 7 (Fig. 3D-F). Therefore, specific amounts of Ring1B, M33
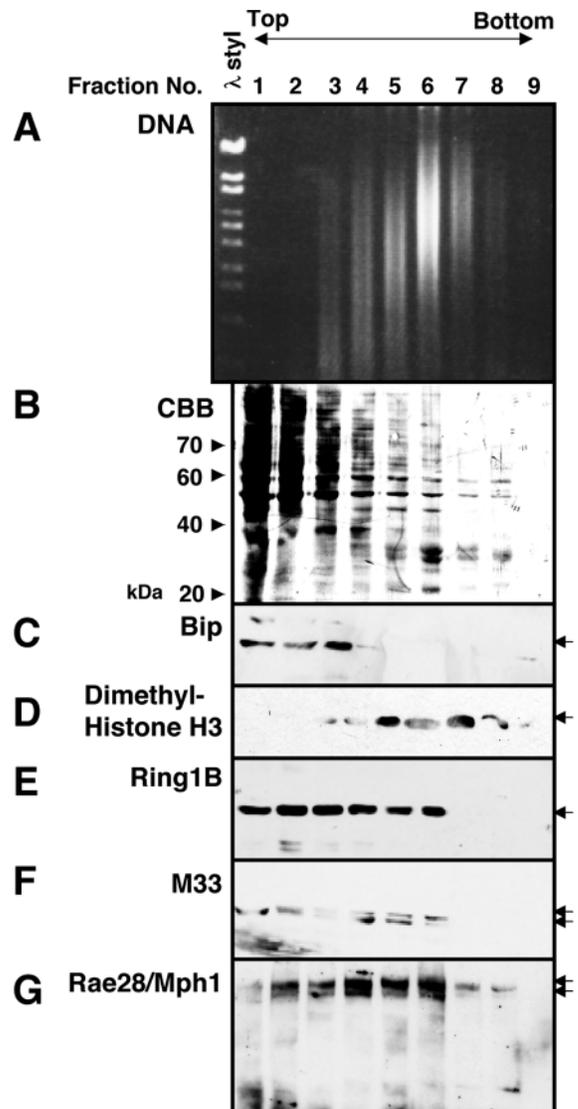


**Fig. 3.** Association of Ring1B, M33 and Rae28/Mph1 with chromosomal DNA. Protein/DNA complex was concentrated by in vivo formaldehyde crosslinking and subsequent cesium chloride isopyknic centrifugation. (A) Chromosomal DNA in each fraction was visualized by Ethidium Bromide staining. λDNA digested with *Sty*I was used as molecular weight markers. (B) Protein in each fraction was visualized by Coomassie Brilliant Blue (CBB) staining. Localization by western blot analysis of an ER luminal protein, Bip (C), dimethyl-Histone H3 (D), Ring1B (E), M33 (F) and Rae28/Mph1 (G).

and Rae28/Mph1 are associated with chromosomal DNA. Indeed, we have found that a significant amount of chromosomal DNA from fraction 6 could be co-immunoprecipitated by antibodies against Ring1B and Rae28/Mph1 (Y. F., unpublished). Our results also indicate that significant amount of Ring1B, M33 and Rae28/Mph1 are not closely associated with chromatin.

## Association of Ring1B to the chromosomal DNA is cell cycle-dependent

It is known that in tissue culture cells RING1 and BMI1-

**Fig. 4.** Subcellular localization of RING1B in interphase and mitotic nuclei. (A,B) Distribution of RING1B and CENPB (A) and centromeric antigens (B) in interphase nucleus of U2-OS cells. (Parts a) Localization of endogenous RING1B (green). (Parts b) Localization of endogenous CENPB (A) and centromeric antigens (B; ACA) (red). (Parts c) DAPI (blue). (Parts d) Merged images. (Parts e) Higher magnification views of the boxed regions in parts d. (C) Distribution of RING1B (part a, green) and CENPB (part b, red) in prophase nucleus of U2-OS cells. (part c) DAPI (blue). (Part d) Merged images. (D) Distribution of RING1B (part a; green) and centromeric antigens (part b; red) in prometaphase nucleus of U2-OS cells. (Part c) DAPI (blue). (Part d) Merged images. (Part E) Distribution of RING1B (part a; green) and CENPB (part b; red) in anaphase nucleus of U2-OS cells. (Part c) DAPI (blue). (Part d) Merged images.
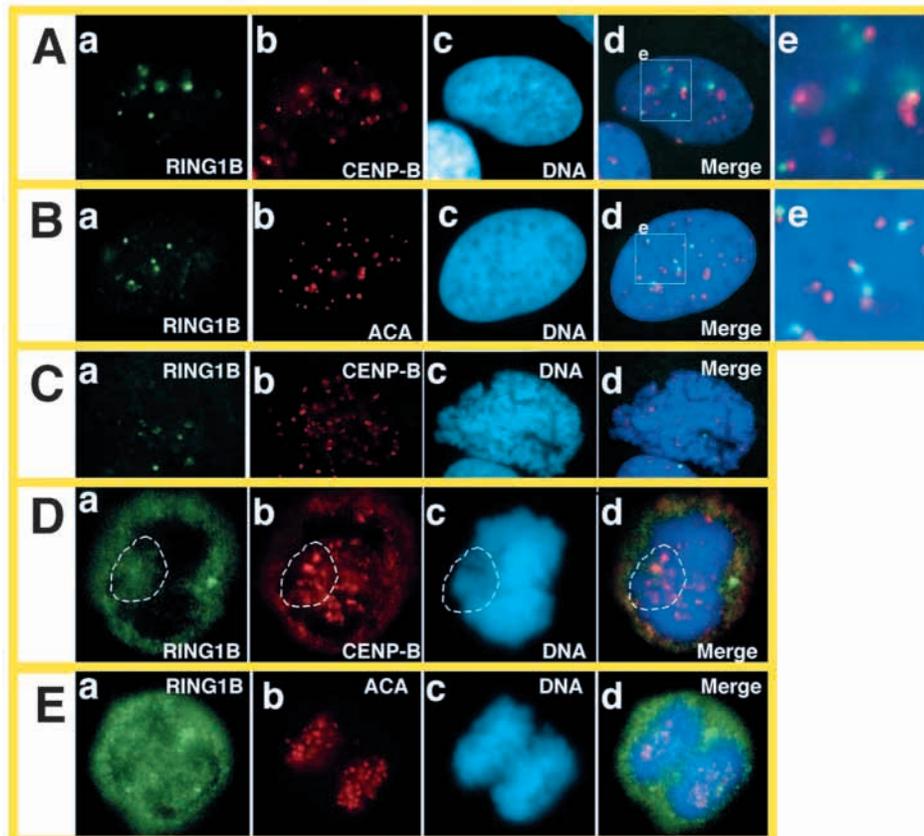


**Fig. 5.** Disruption of the *Ring1B* gene in mice. (A) Diagram of the *Ring1B* locus, the targeting vector and of the modified allele. The *Ring1B*-coding exons are indicated by black boxes. The PGK*neo* and pMC1-*tk* expression cassettes were used for positive and negative selection, respectively. Position of relevant restriction sites (*Eco*RI, E; *Bam*HI, B; *Hin*dIII, H; *Sal*I, S; *Xho*I, X), location of probe and PCR primers, and sizes of diagnostic fragments are indicated. (B) Southern analysis of genomic DNA isolated from offspring of heterozygote matings after digestion with *Bam*HI + *Hin*dIII and probed with the indicated 3′ probe shown in A. (C) PCR analysis of tail genomic DNA of the offspring of a heterozygous intercross. Primers RB22 and RB18 amplify a 1.4 kb of the wild-type allele, whereas primers Neo2 and RB11 amplify a 3.0 kb of the mutated allele. (D) Semi-quantitative analysis of Ring1B by western blot analysis of total proteins extracted from 11.5 dpc mouse embryos of the indicated genotypes probed with antibodies against Ring1B. To correct for loading differences, anti-lamin B antibodies and Coomassie Brilliant Blue (CBB) staining of the same gel were used.
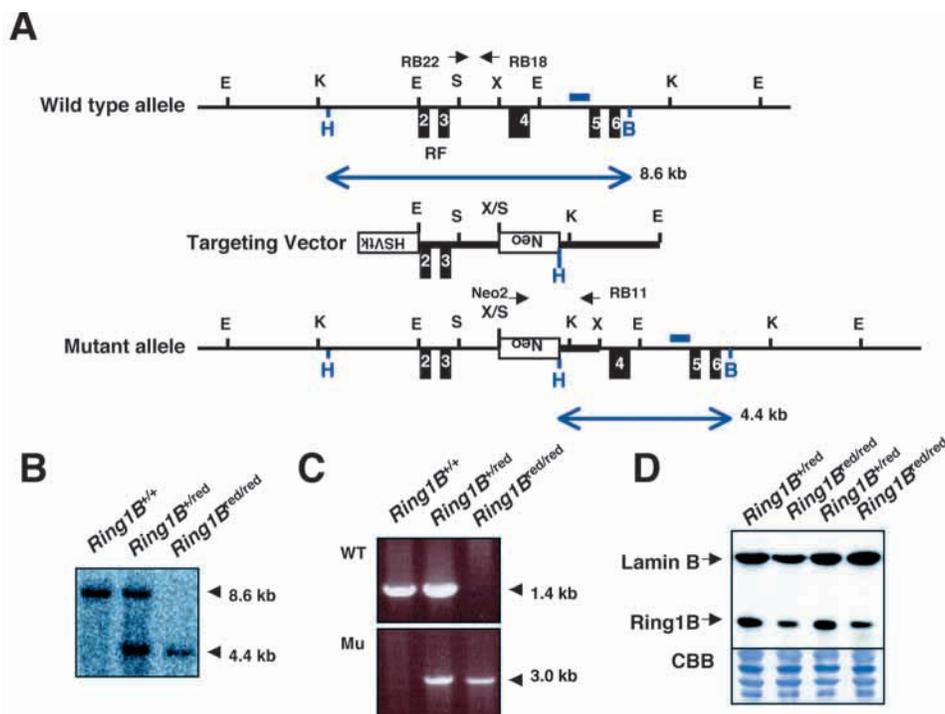
containing PcG bodies associate with pericentromeric heterochromatin in a cell cycle-dependent manner (Saurin et al., 1998). Therefore, we asked what the localization of Ring1B would be during the various phases of the cell cycle. In the interphase nuclei of U2-OS cells, Ring1B showed a speckled distribution associated to centromeric regions, just as it was found for Ring1, Bmi1 and M33 (Fig. 4A,B) (Saurin et al., 1998; Voncken et al., 1999; Wang et al., 1997). At mitosis, the chromosomal signal of Ring1B was very much reduced. However, upon chromosome condensation at prophase, Ring1B proteins were still associated with condensed chromosomes (Fig. 4C). At prometaphase, following disassembly of the nuclear envelop and nuclear matrix, Ring1B staining was significantly weaker to that in interphase nuclei and dispersed into the cytoplasm, although a weak signal was still seen associated with part of pericentromeric chromatin regions (broken line in Fig. 4D). At anaphase, a clearer Ring1B signal was found associated to chromosomal structures, but most of the signal was still found evenly distributed in a speckle-free cytoplasm (Fig. 4E). Thus, the localization of Ring1B at pericentromeric heterochromatin is cell cycle regulated in a similar manner to that of Ring1 or Bmi1 (Saurin et al., 1998; Voncken et al., 1999).

## Generation of a hypomorphic *Ring1B* allele

To start analyzing functionally Ring1B, we tried to inactivate the Ring1B locus in mice. In a gene targeting experiment, we obtained one clone with a modified *Ring1B* locus. Southern blot and sequence analysis of this locus showed that the selectable *Neo* cassette, together with some 0.8 kb sequences in one of the homology arms present in the targeting construct, were unexpectedly inserted between the exons labeled 3 and 4 (Fig. 5A-C). Because no other alterations were observed, there was the possibility that this modified *Ring1B* locus would synthesize an intact protein. We analyzed *Ring1B* gene expression in mice homozygous for the mutation and found that a cDNA encoding the full *Ring1B* ORF could be identified by RT-PCR (data not shown). However, the levels of Ring1B protein in these mice were significantly reduced compared with those in wild-type animals (Fig. 5D). Quantification of Ring1B signals in a Western blot of both homozygous and heterozygous mutant embryos, using the signals of LaminB to normalize for loading differences, showed that the levels of Ring1B in homozygous *Ring1B* mutant embryos were about 30% of those in heterozygous embryos. The reduced levels of Ring1B in the mutant mice, therefore, make it likely that this *Ring1B* allele is a hypomorphic one and is therefore designated
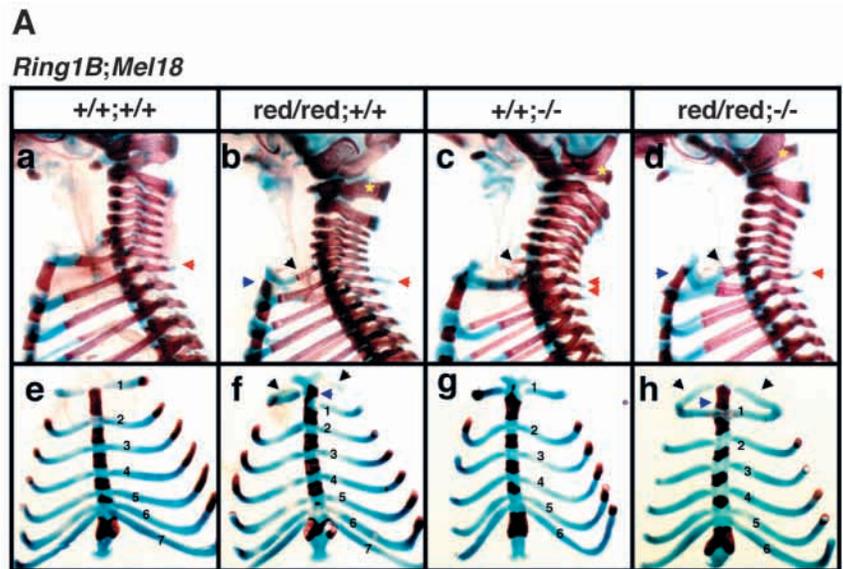


**Fig. 6.** Skeletal alterations of *Ring1B*red/red, *Mel18*–/– and *Ring1B*red/red*Mel18*–/– mice. (A) The genotypes are indicated at the top. (Parts a-d) Lateral views of the upper part of the vertebral column. Yellow stars in parts c and d indicate a ectopic arch of the occipital bone. Black arrows in parts b-d indicate ectopic ribs associated with the 7th cervical vertebra. Red arrows indicate the prominent spinous process. Blue arrows in parts b and d indicate the additional ossification center of the sternum implying the anterior shift of the sternum. (Parts e-h) Ventral views of the rib cages. Black arrows in parts f and h indicate ectopic ribs associated with 7th cervical vertebra. (B) Various posterior transformations of the axial skeleton and their penetrance (indicated in parenthesis): (1) Supraoccipital bone→C1, appearance of the ectopic bones seen in the craniodorsal region of the C1 vertebra or ectopic arch of the occipital bones; (2) C1→C2, presence of the odontoid process on the C1 vertebra; (3) C2→C3, lack of the odontoid process from the C2 vertebra; (4) C7→T1, appearance of cervical ribs on C7; (5) T1→T2, prominent spinous process on T1; (6) T7→T8, dissociation of 7th rib from the sternum; (7) T13→L1, loss of the rib in 20th vertebra; (8) L5 or 6→S1, formation of the sacro-iliac joint in 25th or 26th vertebra; (9) S4→Ca1, appearance of the first caudal vertebra in 29th or 30th vertebra; (10) anterior shift of the sternum as revealed by an ectopic ossification.
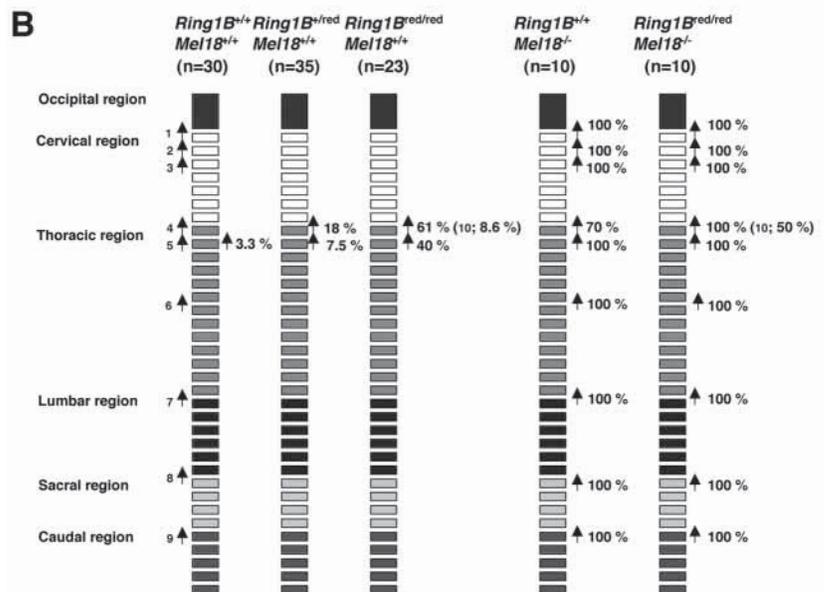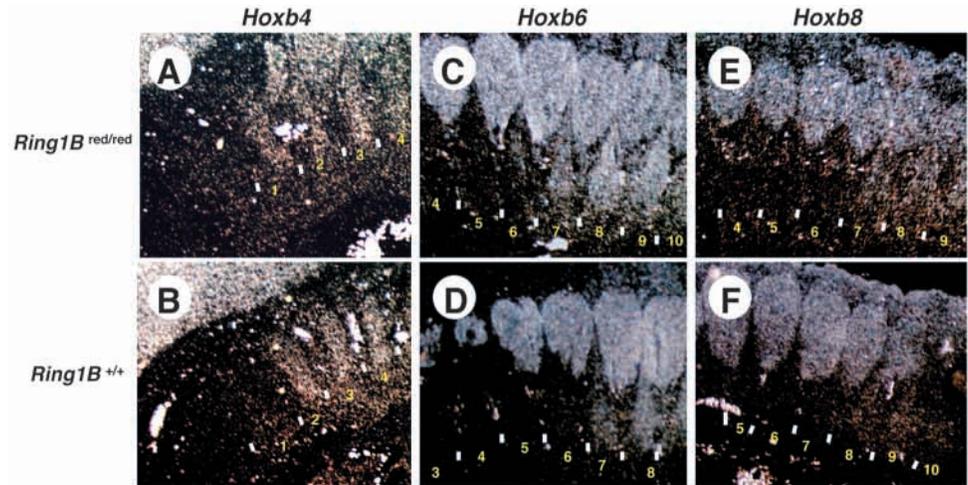
**Fig. 7.** Expression of Hoxb genes in 11.5 dpc wild-type and *Ring1B*<sup>red/red</sup> mutant embryos. Lateral view of sagittal sections showing the expression of *Hoxb4* (A,B), *Hoxb6* (C,D) and *Hoxb8* (E,F) in *Ring1B*<sup>red/red</sup> (A,C,E) and wild type embryos (B,D,F). The number of prevertebrae starting at the proatlas are shown and segment boundaries are indicated by bars.

as *Ring1B*<sup>reduced</sup> (*Ring1B*<sup>red</sup> hereafter). *Ring1B*<sup>red</sup> homozygotes were healthy and fertile.

## Axial skeletal abnormalities and alterations in *Hox* gene expression in *Ring1B*<sup>red/red</sup> mutants

Perturbation of PcG function in mice characteristically results in homeotic transformations and other alterations of the axial skeleton (Akasaka et al., 1996; van der Lugt et al., 1994; Core et al., 1997; Takihara et al., 1997; del Mar Lorente et al., 2000). Therefore, if Ring1B participates in such a function, it is possible that similar defects could be seen in *Ring1B*<sup>red</sup> mice. We found reproducible alterations in the cervicothoracic boundary of the axial skeleton of homozygous *Ring1B*<sup>red</sup> mice, but not wild type. Thus, in 61% of the mice, we found ectopic ribs associated with the 7th cervical (C7) vertebra (Fig. 6A, parts b and f, Fig. 6B). At a lower penetrance, 40% of mice, we found that the prominent spinous process characteristic of the 2nd thoracic vertebrae (T2) was on the T1. These alterations were seen even in heterozygous *Ring1B*<sup>red</sup> mice, although at low frequency (Fig. 6B). Formation of an additional ossification center in the cranial region of the sternum indicated anterior shift of the sternum in *Ring1B*<sup>red</sup> homozygotes (Fig. 6A, part f). Holes in the ossification centers in the upper region of the xyphoid process were observed (Fig. 6A, part f). This is also seen in *Hoxc4* mutants (Saegusa et al., 1996). Thus, these alterations in the axial skeleton and sternum seen in *Ring1B*<sup>red</sup> mice can be interpreted as posteriorizations of the vertebral identities: C7→T1 and T1→T2.

As the anterior boundaries of *Hoxb4, Hoxb6* and *Hoxb8* expression in the paraxial mesoderm demarcate the prospective vertebrae C2, C7 and T1, respectively, we asked whether their expression patterns would be altered in *Ring1B*<sup>red</sup> mice. The analysis of 11.5 dpc embryos homozygous for the *Ring1B*<sup>red</sup> allele showed weak but reproducible signals for *Hoxb4* and *Hoxb8* in the C1 and C7 prevertebrae, respectively, whereas no signals were detected in the wild-type littermates (Fig. 7). Ectopic expression of *Hoxb6* was weakly seen in the prospective neural arch of C6 prevertebra (Fig. 7). The expression of *Hoxb4*, *Hoxb6* and *Hoxb8* in the neural tube was not significantly altered.

Thus, the homeotic transformations of the axial skeleton and the anteriorization of the rostral boundaries of Hox gene

expression in the paraxial mesoderm seen in this hypomorphic *Ring1B* mouse line suggest that Ring1B plays a role in PcG function in mice.

## Genetic interactions between *Ring1B*<sup>red</sup> and *Mel18* null-mutations

To evaluate the involvement of Ring1B in PcG function further, we investigated a possible genetic interaction with *Mel18* by analyzing the axial skeleton of the offspring of crosses of *Ring1B*<sup>red/+</sup>*Mel18*<sup>+/−</sup> mice. *Mel18*<sup>−/−</sup> mice with C57BL/6J genetic background now show a more homogeneous phenotype than when in a hybrid genetic background that we described previously and do not survive birth (Akasaka et al., 1996). The formation of ectopic arches in the occipital bone caused by the ectopic segmentation of the occipital bone, which was not observed in the hybrid genetic background, was now seen in every mouse (Fig. 6A, part c). The C1 vertebra was thinner than that of mice of a mixed genetic background and anterior shifts around the thoracolumbar, lumbosacral and sacrocaudal transition regions were uniformly seen in all *Mel18*<sup>−/−</sup> mice. Interestingly, ectopic ribs on the seventh cervical vertebra were less prominent and penetrant (Fig. 6B).

Animals double homozygous for mutations in the *Ring1B*<sup>red</sup> and *Mel18* loci do not survive birth and showed homogeneous phenotypes, very similar to that of *Mel18*-null mice, except for the cervicothoracic region, in which almost perfect ribs were bilaterally articulated with an anteriorly shifted sternum in 50% of the mice. A unilateral association was seen in 8.6% of *Ring1B*<sup>red/red</sup> and was never seen in *Mel18* null mice (Fig. 6A, part d, part h, Fig. 6B). In summary, the phenotypes at the cervicothoracic level are more severe than the phenotypes of both single mutants in the C57BL/6J background, which provides genetic evidence for an interaction between mutations at the genes encoding *Ring1B* and *Mel18*.

By contrast, the posterior transformations seen in the axial skeleton of *Mel18*<sup>−/−</sup> mice were variably restored in *Ring1B*<sup>red/red</sup>*Mel18*<sup>−/−</sup> mice on the compound background between 129/SvJ derived from R1 ES cells and C57BL/6J, while enhanced phenotypes were also seen with less penetrance (Fig. 8). Double homozygotes were healthy and fertile on the compound background. We found three groups of mice homozygous for both *Ring1B*<sup>red</sup> and *Mel18*, depending

on the alterations in their axial skeletons. One group, comprising about half of the mice (7/15) of the mice showed phenotypes almost identical to those of *Mel18*^{−/−} mice, except for the unilateral association of the seventh rib to the sternum (Fig. 8A, parts f, l and r). A second group, made with the other half of the mice (8/15), showed partial restoration of the posterior homeotic transformations typically seen in *Mel18*^{−/−} to the wild-type phenotype. A representative phenotype of three mice in the latter group is the one shown in Fig. 8A (parts d, j and p). They showed normal occipital bones and C1 vertebra, with seven sternovertebral ribs and normally positioned lumbosacral and sacrocaudal boundaries, and anterior shift the thoracolumabar boundary (as represented by lack of 13th rib) (Fig. 8A, parts d, j and p). Thus, this group exhibited a wild-type axial skeleton, except for the alterations in the thoracolumbar transitional zone. Five mice in the latter group, represented by the specimen shown in Fig. 8A (parts e, k and q) exhibited posterior transformations of the occipital, cervical and upper thoracic regions of the axial skeleton characteristics of *Mel18*^{−/−} mice. However, the lower thoracic, lumbar, sacral and caudal regions had a wild-type appearance. Therefore, the hybrid background does not allow the *Ring1B* mutation to lead to a clearly penetrant patterning defect. It also weakens the penetrance of abnormal phenotypes because of the *Mel18* mutation at specific AP levels, and it leads to a partial rescue of the *Mel18* mutant defects at all AP levels in the compound mutants. Strong interference of strain specific modifiers(s) in the hybrid background probably does not allow for the verification of genetic interaction observed in the C57BL/6.

## Repression of *cHoxb9* expression by overexpression of Ring1B protein

To examine the effect of a gain of function of Ring1B on Hox gene expression, we unilaterally overexpressed it in the developing neural tube of chicken embryos by in ovo electroporation (Fig. 9A, part a). For 0-5 somites embryos, only 10% of transfected embryos survived in our experimental conditions and most of
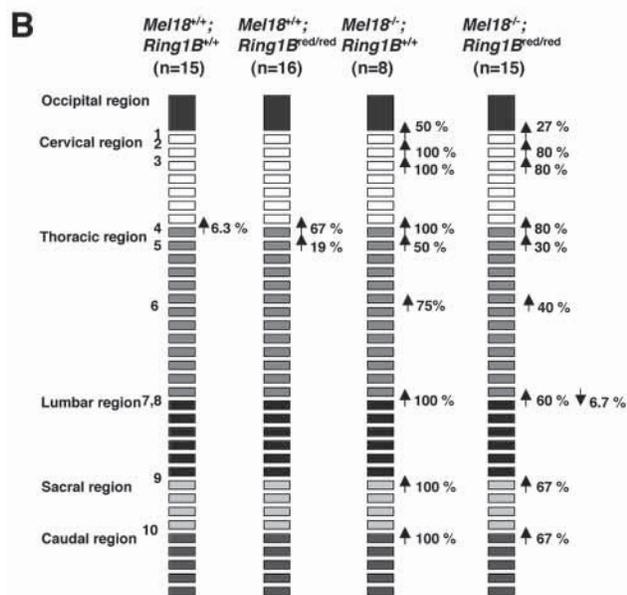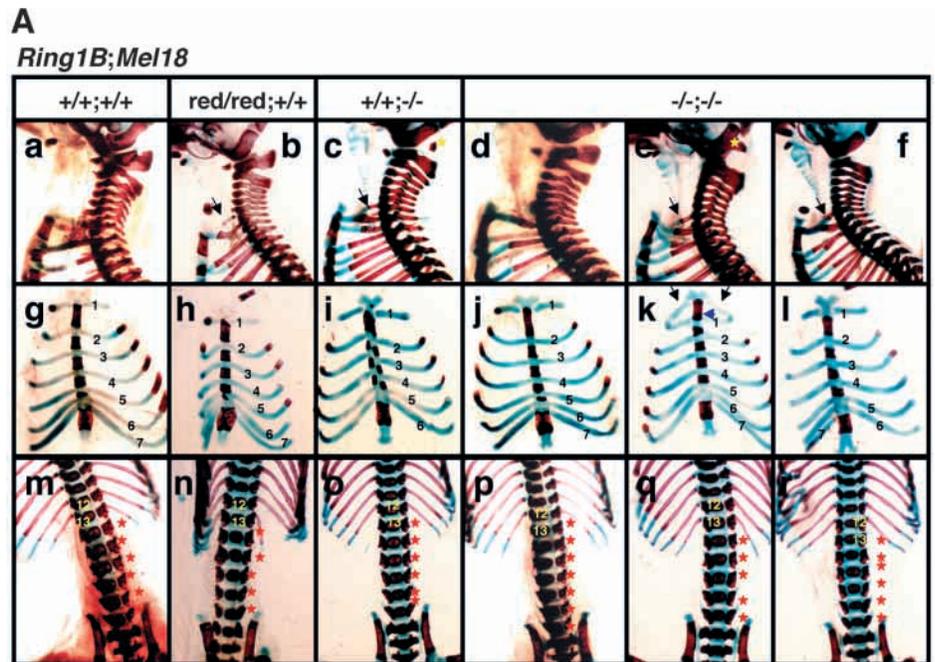


**Fig. 8.** Skeletal alterations seen in *Ring1B*[red/red], *Mel18*^{−/−} and *Ring1B*[red/red]*Mel18*^{−/−} mice on the compound genetic background. (A) Respective genotype of *Ring1B* and *Mel18* loci are indicated at the top. For *Ring1B*[red/red]*Mel18*^{−/−}, three specimens are shown. (Parts a-f) Lateral views of the upper part of the vertebral column are shown. Stars in parts c and e indicate ectopic floating bone or ectopic arch of the occipital bone, respectively. Arrows in parts b, c, e and f indicate ectopic ribs associated with C7. (Parts g-l) Ventral views of the rib cages are shown. In part k, ectopic ossification center of the sternum as a consequence of complete anterior shift of the sternum and complete ectopic ribs are indicated by a blue arrow and black arrows, respectively. Note 7th ribs are articulated with the sternum in *Ring1B*[red/red]*Mel18*^{−/−} mice. (Parts m-r) Ventral views of the thoracolumbar region are shown. Prospective T12 and T13 are indicated by respective numbers. Prospective lumbar vertebrae are indicated by red stars individually. (B) The frequency of the posterior transformations of the axial skeleton is schematically represented. The following parameters are scored and frequency of each alteration is indicated in parentheses: (1) supraoccipital bone→C1, appearance of the ectopic bones seen in the craniodorsal region of the C1 vertebra or ectopic arch of the occipital bones; (2) C1→C2, presence of the odontoid process on the C1 vertebra; (3) C2→C3, lack of the odontoid process from the C2 vertebra; (4) C7→T1, appearance of cervical ribs on C7; (5) T1→T2, prominent spinous process on T1; (6) T7→T8, dissociation of 7th rib from the sternum; (7) T13→L1, loss of the rib on 20th vertebra; (8) L1→T13, appearance of the rib on 21st vertebra; (9) L5 or 6→S1, formation of the sacro-iliac joint in 25th or 26th vertebra; and (10) S4→Ca1, appearance of the first caudal vertebra in 29th or 30th vertebra.

**Fig. 9.** Repression of chicken *Hoxb9* expression by overexpression of mouse Ring1B and Mel18. (A, part a) In ovo electroporation. A pair of electrodes held by a manipulator is inserted through a window and placed over the vitelline membrane overlying the embryo. Plasmid solution colored by Nile Blue is injected into the developing spinal cord as indicated by a yellow bracket. (parts b,c) *Hoxb9* expression in seven-somite (part b) and 15-somite (part c) stage embryos. Somite boundaries are shown. (B, part a) Expression of *mRing1B* 24 hours after electroporation. (parts b-d) Repression of *Hoxb9*
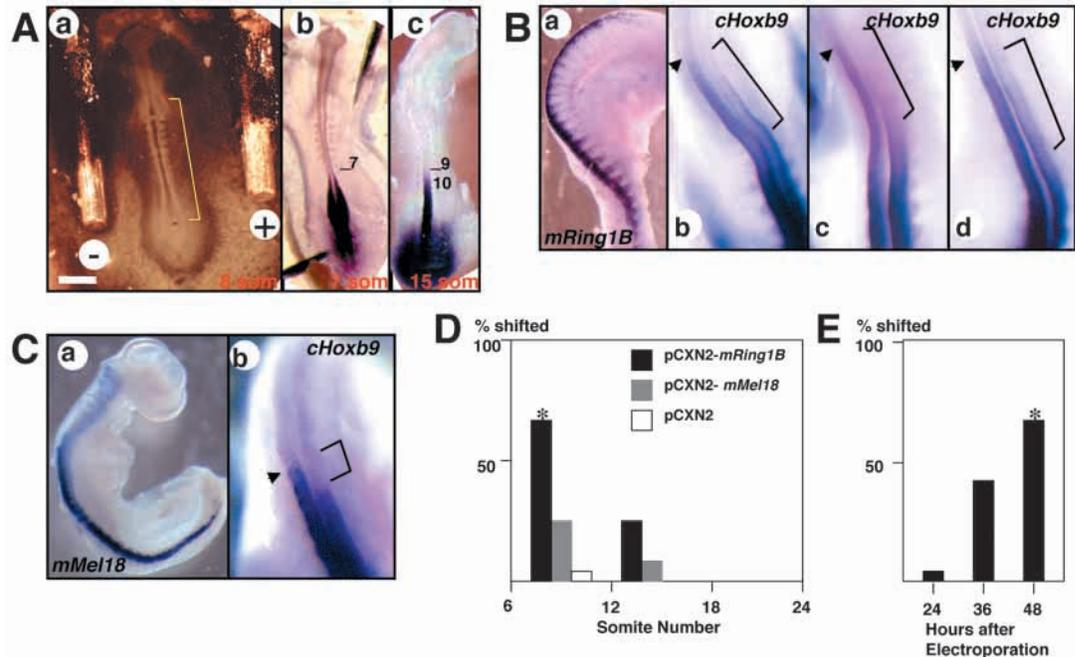


expression observed 48 hours after electroporation. The anterior boundaries of *Hoxb9* expression in the control sides are indicated by arrows. Downregulation of *Hoxb9* expression by exogenous Ring1B are indicated by brackets. (C, part a) Expression of *mMel18* 24 hours after electroporation. (part b) Repression of *cHoxb9* expression 48 hours after electroporation. The anterior boundary of *Hoxb9* expression in the control side is indicated by an arrow. Downregulation of *Hoxb9* expression by mouse *Mel18* is indicated by a bracket. (D) Ring1B- and Mel18-dependent repression of *Hoxb9* expression is influenced by the developmental stage. Frequency of affected embryos by transfection of mouse *Ring1B*, *Mel18* and empty vectors were represented by closed, shaded and open bars, respectively. Mel18-dependent repression is less efficient than that of Ring1B and is similarly influenced by developmental stage. (E) Ring1B-dependent repression of *Hoxb9* expression becomes obvious at least 36 hours after the electroporation. Asterisks in D and E indicate results from the identical series of experiments.

surviving embryos exhibited extensive morphological defects in the neural tube. Thus, we used embryos older than the 6-somite stage. By means of this method, mouse Ring1B and Mel18 were successfully expressed in the developing spinal cord 24 hours after electroporation, but less intensely in the hindbrain (Fig. 9B, part a, Fig. 9C, part a). We investigated the expression of chicken *Hoxb9* in the neural tube because its expression extends up to the level of 9th or 10th somite where stable ectopic expression of mouse *Ring1B* and *Mel18* was seen (Fig. 9A, parts b and c). We first studied the expression of chicken *Hoxb9* gene 48 hours after electroporation of chick embryos of various stages of development. In 6-12 somite embryos, we observed a significant posteriorization of the anterior boundary of chicken *Hoxb9* expression in 67% of efficiently transfected embryos (Fig. 9B,D). The downregulation of chicken *Hoxb9* expression by Ring1B usually extended along several somites (parentheses in Fig. 9B, parts b-d). The introduction of empty vector occasionally resulted in a subtle posteriorization of chicken *Hoxb9* of about half somite width (4%) (Fig. 9D) (M. S., unpublished). The Ring1B-mediated repression of chicken *Hoxb9* expression was much weaker when 12-18 somites embryos were electroporated (only 25% showed a posterior shift) and no effect was seen on 18-24 somite embryos (Fig. 9D). By analyzing embryos at 24, 36 and 48 hours after electroporation, we found it took 36 hours for the repression of chicken *Hoxb9* expression to occur (Fig. 9E).

Similar experiments with Mel18 showed a very mild posteriorization of the anterior boundary of chicken *Hoxb9* expression that affected only a somite in only 25% of the efficiently transfected embryos (Fig. 9C,D).

## DISCUSSION

In this study, we provide ample evidence to indicate that Ring1B is a functional component of mammalian PcG complexes. Thus, co-immunoprecipitation and subnuclear localization studies show that Ring1B is found in protein complexes together with other PcG proteins such as Mel18, M33 and Rae28/Mph1. In addition, a hypomorphic loss-of-function mouse model revealed alterations in the axial skeleton and in the expression pattern of some Hox genes, consistent with a PcG function. Conversely, transient gain-of-function experiments in chick embryos showed a role of Ring1B in the repression of Hox gene expression. Finally we showed a genetic interaction between *Ring1B* and *Mel18* resulting in the enhancement of *Mel18*-deficient phenotypes by the reduction of Ring1B dose on the C57BL/6J background. Taken together, these observations strongly qualify Ring1B as a mammalian PcG gene product.

The phenotype of the *Ring1B* mutant mice described here show some differences with those of mice with mutations in other PcG genes. Thus, the axial skeletal alterations in *Ring1B*[red/red] mice are restricted to the cervicothoracic transitional zone, while they are seen along the entire axis in

other PcG mutant mice (Akasaka et al., 1996; van der Lugt et al., 1994; Core et al., 1997; Takihara et al., 1997; del Mar Lorente et al., 2000). We believe this apparent difference does not imply that Ring1B function is restricted to the prospective cervicothoracic transitional region. First, the mutant mice show a reduction of Ring1B levels, whereas all other PcG mutant mice bear null mutations, and it is possible that specification events in that region are the most sensitive to Ring1B dose. Second, *Ring1B*red/red embryos show a de-repression of *Hoxb4* mesodermal expression in C1 prevertebra. The fact that neither a transformation of cervical vertebrae C1 to C2 nor any other alterations that affect these vertebrae are observed could be explained if the deregulation of other Hox genes required for C1 specification are not significantly affected in *Ring1B*red/red mice. Third, the effect that the low levels of Ring1B has on the phenotype of the axial skeleton of mice lacking Mel18 affects regions throughout the entire axis in hybrid genetic background.

Present and previous biochemical studies indicate that Ring1B is found in protein complexes containing other PcG proteins, such as M33, RYBP, Mel18 and Rae28/Mph1 (Schoorlemmer al., 1997; Garcia et al., 1999). Furthermore, we have shown for the first time that in mammals these PcG proteins are closely associated to chromosomal DNA, as it had been observed before in *D. melanogaster*, while significant quantities of them are not closely associated with chromatin (Zink and Paro, 1989; Orlando and Paro, 1993). Ring1B associates with a PcG multimeric complex through multiple protein-protein interactions, as suggested for other components of PcG complexes (Garcia et al., 1999). We have shown here that Ring1B binds Mel18 and Bmi1 via its N-terminal half, which includes a RING finger motif. However, it has been shown that Ring1B binds M33 and RYBP via C-terminal half (Schoorlemmer et al., 1997; Garcia et al., 1999). The structural similarities of Ring1B-binding domains of Mel18 and Bmi1 (94% identity of amino acids), suggest that they may associate with the same interacting surface on Ring1B. As Mel18 and Bmi1 are known to function redundantly during AP specification and protection against apoptosis, biological impacts might be similar between Ring1B/Mel18 and Ring1B/Bmi1 interactions (Akasaka et al., 2001). However, Hox gene expression is uniquely affected in *Mel18-* and *Bmi1-*deficient mice (Akasaka et al., 1996; van der Lugt et al., 1996). This suggests that Ring1B might preferentially interact with either Mel18 or Bmi1 in Hox gene-dependent manner. This preference could also be influenced by the other components of the PcG complexes as different sets of Hox genes are also affected in *M33-* and *Rae28/Mph1-*deficient mice (Core et al., 1997; Takihara et al., 1997).

Novel genetic interactions between *Ring1B*red and *Mel18-*null mutations upon the compound genetic background suggest the polygenic regulation of mammalian PcG complexes. Restorations of posterior transformations caused by *Mel18* null-mutation by *Ring1B*red mutation suggests presence of compensatory machinery. In particular, Bmi1 could function to compensate *Mel18* mutation. As Bmi1 is known to interact with not only Ring1B but also Rae28/Mph1 and Mph2, multimerization of Bmi1 and its interactors could be modified by unknown polymorphic elements (Hemenway et al., 1998). Molecular basis for genetic modifiers for PcG is not known; however, genes encoding constituents of PcG complex or

proteins required for post-translational modification of PcG proteins could be involved (Voncken et al., 1999).

The repression of chicken *Hoxb9* expression by transient high levels of mouse Ring1B and Mel18 in chicken embryos is in good agreement with the posteriorization of the rostral boundaries of Hox gene expression seen in *Bmi1* and *Ring1A* transgenic mice (Alkema et al., 1995; del Mar Lorente et al., 2000). These data are also consistent with previous observations that most PcG proteins, including Ring1 family proteins act as transcriptional repressors when recruited to reporter constructs (Satijn et al., 1997b; Schoorlemmer et al., 1997). The anterior boundary of chicken *Hoxb9* expression in the neural tube at the level of prospective 9th somite is already established in seven-somite embryos (Fig. 9A, part b). Thus, the overexpression of mouse Ring1B and Mel18 results in the active silencing of a chicken *Hoxb9* gene, which is already transcriptionally active. Such an effect may result from the recruiting of ectopic Ring1B and Mel18 to regulatory regions of chicken *Hoxb9*, which, in turn, may alter locally the structure of the chromatin. However, overexpression of Ring1B does not affect chicken *Hoxb9* expression in later stage embryos (Fig. 8C). Biochemical studies using purified PcG complexes and chromatin remodeling factors of the SWI/SNF provide clues on how PcG and trxG proteins counteract (Shao et al., 1999). PcG complexes act as a molecular lock when tethered on nucleosomes prior to exposure to the remodeling factors. Conversely, once exposed to SWI/SNF factors, PcG-mediated repression does not occur. If this is the case, the inability of Ring1B to repress chicken *Hoxb9* expression at later stages in development may be due to the establishment of a trxG-dependent activation of chicken *Hoxb9*. Thus, the accessibility to, or the activity of Ring1B-containing PcG complexes on Hox clusters might be regulated in a developmental stage-dependent manner, as suggested in *D. melanogaster* (Orlando et al., 1998).

## REFERENCES

**Akasaka, T., Kanno, M., Balling, R., Mieza, M. A., Taniguchi, M. and Koseki, H.** (1996). A role for mel-18, a Polycomb group-related vertebrate gene, during theanteroposterior specification of the axial skeleton. *Development* **122**, 1513-1522.

**Akasaka, T., van Lohuizen, M., van der Lugt, N., Mizutani-Koseki, Y., Kanno, M., Taniguchi, M., Vidal, M., Alkema, M., Berns, A. and Koseki, H.** (2001). Mice doubly deficient for the Polycomb Group genes Mel18 and

Bmi1 reveal synergy and requirement for maintenance but not initiation of Hox gene expression. *Development* **128**, 1587-1597.

**Alkema, M. J., van der Lugt, N. M., Bobeldijk, R. C., Berns, A. and van Lohuizen, M.** (1995). Transformation of axial skeleton due to overexpression of bmi-1 in transgenic mice. *Nature* **374**, 724-727.

**Alkema, M. J., Bronk, M., Verhoeven, E., Otte, A., van't Veer, L. J., Berns, A. and van Lohuizen, M.** (1997). Identification of Bmi1-interacting proteins as constituents of a multimeric mammalian polycomb complex. *Genes Dev.* **11**, 226-240.

**Atsuta, T., Fujimura, S., Moriya, H., Vidal, M., Akasaka, T. and Koseki, H.** (2001). Production of monoclonal antibodies against mammalian Ring1B proteins. *Hybridoma* **20**, 43-46.

**Bel, S., Core, N., Djabali, M., Kieboom, K., van der Lugt, N., Alkema, M. J. and van Lohuizen, M.** (1998). Genetic interactions and dosage effects of Polycomb group genes in mice. *Development* **125**, 3543-3551.

**Core, N., Bel, S., Gaunt, S. J., Aurrand-Lions, M., Pearce, J., Fisher, A. and Djabali, M.** (1997). Altered cellular proliferation and mesoderm patterning in Polycomb-M33-deficient mice. *Development* **124**, 721-729.

**del Mar Lorente, M., Marcos-Gutierrez, C., Perez, C., Schoorlemmer, J., Ramirez, A., Magin, T. and Vidal, M.** (2000). Loss- and gain-of-function mutations show a polycomb group function for Ring1A in mice. *Development* **127**, 5093-5100.

**Fields, S. and Bartel, P. L.** (2001). The two-hybrid system. A personal view. *Methods Mol. Biol.* **177**, 3-8.

**Franke, A., DeCamillis, M., Zink, D., Cheng, N., Brock, H. W. and Paro, R.** (1992). Polycomb and polyhomeotic are constituents of a multimeric protein complex in chromatin of Drosophila melanogaster. *EMBO J.* **11**, 2941-2950.

**Garcia, E., Marcos-Gutierrez, C., del Mar Lorente, M., Moreno, J. C. and Vidal, M.** (1999). RYBP, a new repressor protein that interacts with components of the mammalian Polycomb complex, and with the transcription factor YY1. *EMBO J.* **18**, 3404-3418.

**Gebuhr, T. C., Bultman, S. J. and Magnuson, T.** (2000). Pc-G/trx-G and the SWI/SNF connection: developmental gene regulation through chromatin remodeling. *Genesis* **26**, 189-197.

**Gething, M. J.** (1999). Role and regulation of the ER chaperone BiP. *Semin. Cell. Dev. Biol.* **10**, 465-472.

**Gunster, M. J., Satijn, D. P., Hamer, K. M., den Blaauwen, J. L., de Bruijn, D., Alkema, M. J., van Lohuizen, M., van Driel, R. and Otte, A. P.** (1997). Identification and characterization of interactions between the vertebrate polycomb-group protein BMI1 and human homologs of polyhomeotic. *Mol. Cell. Biol.* **17**, 2326-2335.

**Hemenway, C. S., Halligan, B. W. and Levy, L. S.** (1998). The Bmi-1 oncoprotein interacts with dinG and MPh2: the role of RING finger domains. *Oncogene* **16**, 2541-2547.

**Hemenway, C. S., Halligan, B. W., Gould, G. C. and Levy, L. S.** (2000). Identification and analysis of a third mouse Polycomb gene, MPc3. *Gene* **242**, 31-40.

**Jurgens, G.** (1985). A group of genes controlling spatial expression of the bithorax complex in Drosophila. *Nature* **316**, 153-155.

**Kessel, M. and Gruss, P.** (1991). Homeotic transformations of murine vertebrae and concomitant alteration of Hox codes induced by retinoic acid. *Cell* **67**, 89-104.

**Kitagawa, K., Masumoto, H., Ikeda, M. and Okazaki, T.** (1995). Analysis of protein-DNA and protein-protein interactions of centromere protein B (CENP-B) and properties of the DNA-CENP-B complex in the cell cycle. *Mol. Cell. Biol.* **15**, 1602-1612.

**Laible, G., Wolf, A., Dorn, R., Reuter, G., Nislow, C., Lebersorger, A., Popkin, D., Pillus, L. and Jenuwein, T.** (1997). Mammalian homologues of the Polycomb-group gene Enhancer of zeste mediate gene silencing in Drosophila heterochromatin and at S. cerevisiae telomeres *EMBO J.* **16**, 3219-3232.

**Nagy, A., Rossant, J., Nagy, R., Abramow-Newerly, W. and Roder, J. C.** (1993). Derivation of completely cell culture-derived mice from early-passage embryonic stem cells. *Proc. Natl. Acad. Sci. USA* **90**, 8424-8428.

**Nakamura, H. and Funahashi, J.** (2001). Introduction of DNA into chick embryos by in Ovo electroporation. *Methods* **24**, 43-48.

**Nakayama, J., Rice, J. C., Strahl, B. D., Allis, C. D. and Grewal, S. I.** (2001). Role of histone H3 lysine 9 methylation in epigenetic control of heterochromatin assembly. *Science* **292**, 110-113.

**Niwa, H., Yamamura, K. and Miyazaki, J.** (1991). Efficient selection for high-expression transfectants with a novel eukaryotic vector. *Gene* **108**, 193-199.

**Nomura, M., Takihara, Y. and Shimada, K.** (1994). Isolation and characterization of retinoic acid-inducible cDNA clones in F9 cells: one of the early inducible clones encodes a novel protein sharing several highly homologous regions with a Drosophila polyhomeotic protein. *Differentiation* **57**, 39-50.

**Orlando, V. and Paro, R.** (1993). Mapping Polycomb-repressed domains in the bithorax complex using in vivo formaldehyde cross-linked chromatin. *Cell* **75**, 1187-1198.

**Orlando, V., Strutt, H. and Paro, R.** (1997). Analysis of chromatin structure by in vivo formaldehyde cross-linking. *Methods* **11**, 205-214.

**Orlando, V., Jane, E. P., Chinwalla, V., Harte, P. J. and Paro, R.** (1998). Binding of trithorax and Polycomb proteins to the bithorax complex: dynamic changes during early Drosophila embryogenesis. *EMBO J.* **17**, 5141-5150.

**Paro, R.** (1995). Propagating memory of transcriptional states. *Trends Genet.* **11**, 295-297.

**Pearce, J. J., Singh, P. B. and Gaunt, S. J.** (1992). The mouse has a Polycomb-like chromobox gene. *Development* **114**, 921-929.

**Pirotta, V.** (1997). PcG complexes and chromatin silencing. *Curr. Opin. Gent. Dev.* **7**, 249-258.

**Saegusa, H., Takahashi, N., Noguchi, S. and Suemori, H.** (1996). Targeted disruption in the mouse Hoxc-4 locus results in axial skeleton homeosis and malformation of the xiphoid process. *Dev. Biol.* **174**, 55-64.

**Sakamoto, K., Nakamura, H., Takagi, M., Takeda, S. and Katsube, K.** (1998). Ectopic expression of lunatic Fringe leads to downregulation of Serrate-1 in the developing chick neural tube; analysis using in ovo electroporation transfection technique. *FEBS Lett.* **426**, 337-341.

**Satijn, D. P., Olson, D. J., van der Vlag, J., Hamer, K. M., Lambrechts, C., Masselink, H., Gunster, M. J., Sewalt, R. G., van Driel, R. and Otte, A. P.** (1997a). Interference with the expression of a novel human polycomb protein, hPc2, results in cellular transformation and apoptosis. *Mol. Cell. Biol.* **17**, 6076-6086.

**Satijn, D. P., Gunster, M. J., van der Vlag, J., Hamer, K. M., Schul, W., Alkema, M. J., Saurin, A. J., Freemont, P. S., van Driel, R. and Otte, A. P.** (1997b). RING1 is associated with the polycomb group protein complex and acts as a transcriptional repressor. *Mol. Cell. Biol.* **17**, 4105-4113.

**Saurin, A. J., Shiels, C., Williamson, J., Satijn, D. P., Otte, A. P., Sheer, D. and Freemont, P. S.** (1998). The human polycomb group complex associates with pericentromeric heterochromatin to form a novel nuclear domain. *J. Cell Biol.* **142**, 887-898.

**Saurin, A. J., Shao, Z., Erdjument-Bromage, H., Tempst, P. and Kingston, R. E.** (2001). A Drosophila Polycomb group complex includes Zeste and dTAFII proteins. *Nature* **412**, 655-660

**Schoorlemmer, J., Marcos-Gutierrez, C., Were, F., Martinez, R., Garcia, E., Satijn, D. P., Otte, A. P. and Vidal, M.** (1997). Ring1A is a transcriptional repressor that interacts with the Polycomb-M33 protein and is expressed at rhombomere boundaries in the mouse hindbrain. *EMBO J.* **16**, 5930-5942.

**Schumacher, A., Faust, C. and Magnuson, T.** (1996). Positional cloning of a global regulator of anterior-posterior patterning in mice. *Nature* **384**, 648-651.

**Sewalt, R. G., van der Vlag, J., Gunster, M. J., Hamer, K. M., den Blaauwen, J. L., Satijn, D. P., Hendrix, T., van Driel, R. and Otte, A. P.** (1998). Characterization of interactions between the mammalian polycomb-group proteins Enx1/EZH2 and EED suggests the existence of different mammalian polycomb-group protein complexes. *Mol. Cell. Biol.* **18**, 3586-3595.

**Shao, Z., Raible, F., Mollaaghababa, R., Guyon, J. R., Wu, C. T., Bender, W. and Kingston, R. E.** (1999). Stabilization of chromatin structure by PRC1, a Polycomb complex. *Cell* **98**, 37-46.

**Tagawa, M., Sakamoto, T., Shigemoto, K., Matsubara, H., Tamura, Y., Ito, T., Nakamura, I., Okitsu, A., Imai, K. and Taniguchi, M.** (1990). Expression of novel DNA-binding protein with zinc finger structure in various tumor cells. *J. Biol. Chem.* **265**, 20021-20026.

**Takihara, Y., Tomotsune, D., Shirai, M., Katoh-Fukui, Y., Nishii, K., Motaleb, M. A., Nomura, M., Tsuchiya, R., Fujita, Y., Shibata, Y., Higashinakagawa, T. and Shimada, K.** (1997). Targeted disruption of the mouse homologue of the Drosophila polyhomeotic gene leads to altered anteroposterior patterning and neural crest defects. *Development* **124**, 3673-3682.

**Tomotsune, D., Shirai, M., Takihara, Y. and Shimada, K.** (2000). Regulation of Hoxb3 expression in the hindbrain and pharyngeal arches by rae28, a member of the mammalian Polycomb group of genes. *Mech. Dev.* **98**, 165-169.

**van der Lugt, N. M., Domen, J., Linders, K., van Roon, M., Robanus-**

**Maandag, E., te Riele, H., van der Valk, M., Deschamps, J., Sofroniew, M., van Lohuizen, M. and Berns, A.** (1994). Posterior transformation, neurological abnormalities, and severe hematopoietic defects in mice with a targeted deletion of the bmi-1 proto-oncogene. *Genes Dev.* **8**, 757-769.

**van der Lugt, N. M., Alkema, M., Berns, A. and Deschamps, J.** (1996). The Polycomb-group homolog Bmi-1 is a regulator of murine Hox gene expression. *Mech. Dev.* **58**, 153-164.

**van der Vlag, J. and Otte, A. P.** (1999). Transcriptional repression mediated by the human polycomb-group protein EED involves histone deacetylation. *Nat. Genet.* **23**, 474-478.

**van Lohuizen, M., Verbeek, S., Scheijen, B., Wientjens, E., van der Gulden, H. and Berns, A.** (1991). Identification of cooperating oncogenes in E mu-myc transgenic mice by provirus tagging. *Cell* **65**, 737-752.

**van Lohuizen, M., Tijms, M., Voncken, J. W., Schumacher, A., Magnuson, T. and Wientjens, E.** (1998). Interaction of mouse polycomb-group (Pc-G) proteins Enx1 and Enx2 with Eed: indication for separate Pc-G complexes. *Mol. Cell. Biol.* **18**, 3572-3579.

**Vojtek, A. B., Hollenberg, S. M. and Cooper, J. A.** (1993). Mammalian Ras interacts directly with the serine/threonine kinase Raf. *Cell* **74**, 205-214.

**Voncken, J. W., Schweizer, D., Aagaard, L., Sattler, L., Jantsch, M. F. and van Lohuizen, M.** (1999). Chromatin-association of the Polycomb group protein BMI1 is cell cycle-regulated and correlates with its phosphorylation status. *J. Cell. Sci.* **112**, 4627-4639.

**Wang, G., Horsley, D., Ma, A., Otte, A. P., Hutchings, A., Butcher, G. W. and Singh, P. B.** (1997). M33, a mammalian homologue of Drosophila Polycomb localises to euchromatin within interphase nuclei but is enriched within the centromeric heterochromatin of metaphase chromosomes. *Cytogenet. Cell Genet.* **78**, 50-55.

**Wilkinson, D. G. and Nieto, M. A.** (1993). Detection of messenger RNA by in situ hybridization to tissue sections and whole mounts. *Methods Enzymol.* **225**, 361-373.

**Yoda, K., Nakamura, N., Masumoto, H., Suzuki, N., Kitagawa, K., Nakano, M., Shinjo, A. and Okazaki, T.** (1996). A human centromere protein, CENP-B, has a DNA binding domain containing four potential alpha helices at the NH2 terminus, which is separable from dimerizing activity. *Mol. Cell. Biol.* **16**, 5169-5177.

**Zink, B. and Paro, R.** (1989). In vivo binding pattern of a trans-regulator of homoeotic genes in Drosophila melanogaster. *Nature* **337**, 468-471.